DINAME 2019 - Proceedings of the XVIII International Symposium on Dynamic Problems of Mechanics,
M.A. Savi, T.G. Ritto and W.M. Bessa (Editors), ABCM, Buzios, RJ, Brazil, March 10th to 15th, 2019

Orientation Control of a Pan-Tilt Camera Mechanism For Tracking a Moving Target

Alessandro Rosa Lopes Zachi[1,2], Daniela Azevedo Araujo[1], Antonio Candea Leite[3], Josiel Alves Gouvea[2] and Cristiano de Souza Carvalho[2]

Centro Federal de Educação Tecnológica Celso Suckow da Fonseca (CEFET/RJ)

[1] Laboratory of Control Systems and Automation - LACEA
Avenida Maracanã 229, Maracanã - 20.271-110 - Rio de Janeiro, Brazil.

[2] Research Nucleous on Mechatronics - NUPEM
Estrada de Adrianópolis 1317, Santa Rita, Nova Iguaçu - 26.041-271 - Rio de Janeiro, Brazil.

[3] Pontifical Catholic University of Rio de Janeiro (PUC-Rio) - Department of Electrical Engineering (DEE)
Rua Marquês de São Vicente 225, Gávea. CEP 22.451-900 - Rio de Janeiro, RJ - Brazil.

Abstract: In this work, an algorithm based on visual feedback is developed to control the orientation of a pan-tilt camera. The scheme is applied to a servo system consisting of a single fixed-base monocular camera. The key idea is to set the camera orientation automatically, commanding the pan and tilt angles of its base so that a desired (fixed) image point remains focused on the projection of a moving target of interest. The approach focuses attention on designing control laws to drive the DC motors that perform the adequate pan and tilt movements to track the target on-line. To deal with the parametric uncertainties that may occur in the dynamical equations of the system camera-motors, a modified version of the Active Disturbance Rejection Control Method- ADRC is developed. The proposed methodology is used in the mathematical formulation of an output feedback controller whose closed-loop stability analysis can be performed using classical formalism. From a theoretical point of view, the efficiency of the control algorithm is guaranteed by the demonstration of local stability properties and the asymptotic convergence of position errors to a small residual set around zero. In addition, it is demonstrated that the proposed control law does not require the measurements of the pan and tilt angles of the motors and does not depend on the exact knowledge of the intrinsic parameters of the camera-motors mechanism. From a practical point of view, it is believed that the proposed scheme has an attractive advantage for the experimental setup since the implementation of the algorithm does not require neither additional sensors nor the calibration of the camera parameters. The efficiency of the closed-loop visual servoing algorithm is verified through computational simulations.

Keywords: Visual servoing, Pan-Tilt camera, Orientation control, ADRC method.

INTRODUCTION

In the last decades, the computer vision has become an important tool for sensing in robotic systems and applications. The amount of scientific research in this area has grown in large part through the advancement of camera-building technologies and the emergence of various imaging algorithms and programs. Among the most important tasks performed in a computer vision system are procedures for extraction, characterization and interpretation of information from two-dimensional or three-dimensional images of an object or a scene of interest. Recently, this technological tool has been used in numerous real-world applications, such as autonomous robot navigation (Bista *et al.*, 2017), in industrial process control (Vijayan and Ashok, 2017) in surgical medicine (Feng *et al.*, 2018), as well as for rehabilitation (He *et al.*, 2017) in surveillance and security systems, in monitoring systems (Sivčev *et al.*, 2018), and in the military area (Paucar *et al.*, 2018). Another interesting application is related to the use of pan-tilt cameras embedded in vehicles and/or gyro-stabilized platforms for maintain and control the line of sight of an object in relation to another object or inertial space (Masten, 2008). On the other hand, in electro-optical imaging systems, the objective can be only to position the camera or the visual sensor in predefined directions and orientations or surveillance regions, rather than considering the tracing of a specific target (Masten, 2008; Li *et al.*, 2013).

PROBLEM STATEMENT

In this work, we consider the orientation control problem of a fixed base pan-tilt camera to track a moving object in the workspace using only the captured image information. The central idea consists in guiding the camera automatically, that is, by designing the control laws for the pan and tilt angles of the base, so that the image of the projected object on the screen remains focused at the projection of the object. Figure 1 shows a schematic diagram of the control problem considered in this paper.

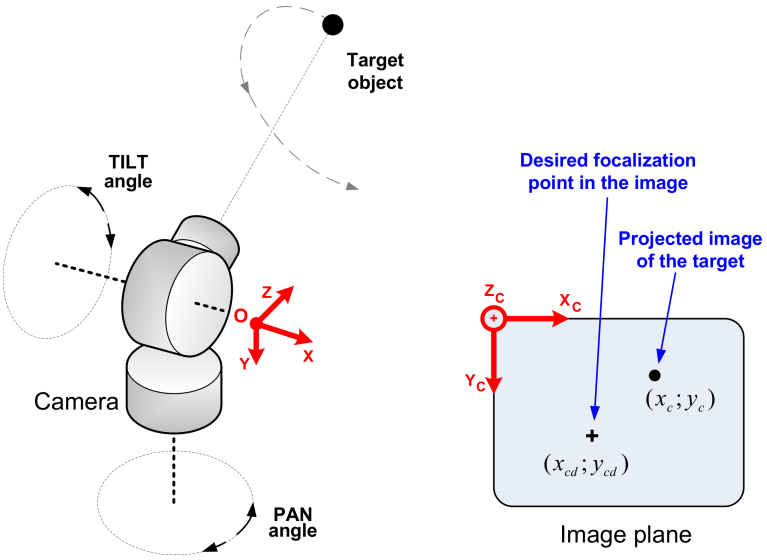

Figure 1 – Schematic block diagram of the pan-tilt visual servoing system.

METHODOLOGY ADOPTED

For solving the control problem stated previously, the Active Disturbance Rejection Method (ADRC) (Han, 1998; Madoński *et al.*, 2015) is adopted. The motivation for the use of ADRC technique in the present work is mainly because of its ability of disturbance rejection and its lack of requirement on the detailed mathematical model of the plant (Madoński *et al.*, 2015). The linear version of the ADRC method consists basically of an extended state observer (ESO) that estimates the system states and non-measurable signals together with a state feedback control law in standard form. As can be seen from the basic design procedures discussed in (Chen *et al.*, 2014; Madoński *et al.*, 2015), the controller implementation is dependent on the knowledge of the plant control coefficient (or control gain), which may be difficult to carry out in the case of plants with parametric uncertainties. In (Zhao and Huang, 2012), the linear version of the standard ADRC strategy proposed by (Han, 1998) was implemented in systems with unknown order and uncertain relative degrees. Besides that, a new robustness analysis considering uncertain control gains was discussed, and some computational simulations were presented.

In this work, we propose some modifications on the input/output dynamics of the plant that brings some mathematics advantages to the closed loop control design, which contrasts with the basic method adopted recently in (Zhao and Huang, 2012; Chen *et al.*, 2014; Madoński *et al.*, 2015) and in (Zhao and Huang, 2012).

SYSTEM MODEL

The Pan-Tilt mechanism considered in this paper is composed of two DC motors for driving the pan and tilt angles of a CCD camera. The physical connections of the system components and signals are depicted in Fig. 2. As it is intended to describe the behavior of the plant from the applied input voltages to the image coordinates of the target, a brief review on the overall system dynamics will be carried out in the following.

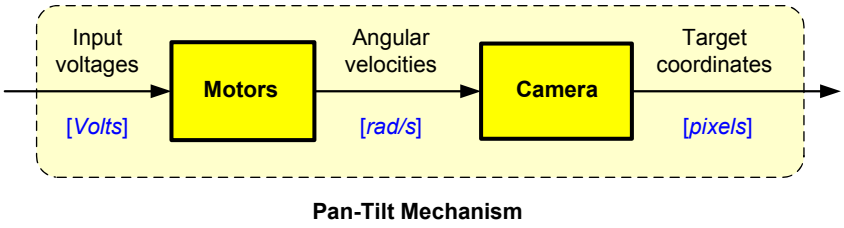

Figure 2 – System overview.

Camera projection model

In this work, we consider the mathematical model proposed in (Hutchinson *et al.*, 1996; Flandin *et al.*, 2000; Kelly *et al.*, 2000) which is generalized to a mobile camera. Since a CCD camera is used to measure the target position, its projection model, which is depicted in Fig.3, need to be included in the system equation.

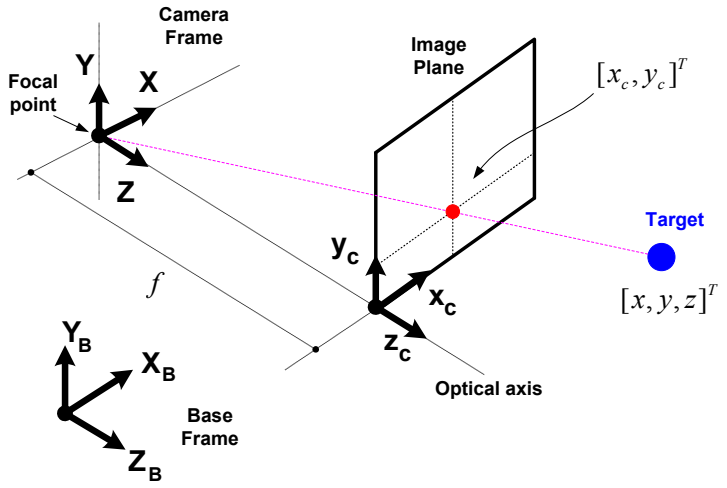

Figure 3 – Camera projection model.

In this paper, the base of the camera is fixed in the workspace and only the Pant and Tilt rotating motions are considered. The origin of the camera coordinate frame with respect to the base frame is represented by $s_c \in \mathbb{R}^3$. The orientation of the camera frame with respect to the base frame is denoted by $R_c \in SO(3)$. The target object, with coordinates $[x,y,z]^T$ in the camera frame, produces a projection point $\mathbf{p_c} = [x_c, y_c]^T \in \mathbb{R}^2$ on the image plane. Let us define $s_o \in \mathbb{R}^3$ as the coordinates of the target object with respect to the base frame. Therefore, the relative position of this object located in the workspace with respect to the camera coordinate frame is $[x,y,z]^T$. According to the perspective projection (Hutchinson *et al.*, 1996; Flandin *et al.*, 2000; Kelly *et al.*, 2000) method, the image point depends uniquely on the object position and on the camera position and orientation, and can be represented by

$$\mathbf{p_c} = \begin{bmatrix} x_c \\ y_c \end{bmatrix} = \frac{\alpha f}{z} \begin{bmatrix} x \\ y \end{bmatrix}, \tag{1}$$

in which $f \in \mathbb{R}$ represents the focal length of the camera (in meters), $z \in \mathbb{R}$ the relative depth distance between the object and the camera (in meters), measured in the direction of its optical axis ($z \gg f$), $\alpha \in \mathbb{R}$ is the camera scaling factor (in pixel/meter). By taking the time derivative of Eq. (1), we obtain:

$$\dot{\mathbf{p}}_\mathbf{c} = \begin{bmatrix} \dot{x}_c \\ \dot{y}_c \end{bmatrix} = \frac{\alpha f}{z} \begin{bmatrix} 1 & 0 & -x/z \\ 0 & 1 & -y/z \end{bmatrix} \begin{bmatrix} \dot{x} \\ \dot{y} \\ \dot{z} \end{bmatrix}. \tag{2}$$

The position of the target with respect to the camera frame is given by

$$\begin{bmatrix} x \\ y \\ z \end{bmatrix} = R_c(s_o - s_c). \tag{3}$$

Since the camera orientation is not static, its rotating motions will affect the dynamics of the target image projection. Thus, by using the well-known general formula for velocity of a moving point in a moving frame with respect to a fixed frame (Hutchinson *et al.*, 1996; Siciliano *et al.*, 2008), it is possible to derive the time derivative of Eq. (3) in terms of the camera translational and angular velocities as (Kelly *et al.*, 2000):

$$\begin{bmatrix} \dot{x} \\ \dot{y} \\ \dot{z} \end{bmatrix} = \begin{bmatrix} 1 & 0 & 0 & 0 & -z & y \\ 0 & 1 & 0 & z & 0 & -x \\ 0 & 0 & 1 & -y & x & 0 \end{bmatrix} \begin{bmatrix} v_c(t) \\ \omega_c(t) \end{bmatrix}, \tag{4}$$

in which $v_c(t) = [v_x,\ v_y,\ v_z]^T \in \mathbb{R}^3$ and $\omega_c(t) = [\omega_x,\ \omega_y,\ \omega_z]^T \in \mathbb{R}^3$ stand for the camera translational and angular velocities with respect to the base frame, respectively. The motion of the target image point as a function of the camera velocities is obtained by replacing Eq. (3) into Eq. (2)

$$\dot{\mathbf{p}}_\mathbf{c} = \frac{\alpha f}{z} \begin{bmatrix} 1 & 0 & -x/z & -xy/z & (x^2+z^2)/z^2 & -y \\ 0 & 1 & -y/z & -(y^2+z^2)/z^2 & xy/z & x \end{bmatrix} \begin{bmatrix} v_c(t) \\ \omega_c(t) \end{bmatrix}. \tag{5}$$

So, in image coordinates, Eq. (5) can be rewritten as

$$\dot{\mathbf{p}}_\mathbf{c} = \begin{bmatrix} \alpha f/z & 0 & -x_c/z & -x_c y_c/\alpha f & [x_c^2+(\alpha f)^2]/\alpha f & -y_c \\ 0 & \alpha f/z & -y_c/z & -[y_c^2+(\alpha f)^2]/\alpha f & x_c y_c/\alpha f & x_c \end{bmatrix} \begin{bmatrix} v_c(t) \\ \omega_c(t) \end{bmatrix}. \tag{6}$$

Assuming that the origins of the camera and base frames are coincident and their coordinated systems have the same orientation, then it is not difficult to verify that the camera translational velocity vector $v = [v_x,\ v_y,\ v_z]^T \equiv [0,\ 0,\ 0]^T$. In such configuration, the camera orientation angles around X_B and Y_B axis coincide, respectively, with the Tilt and Pan angles of the mechanism while the angle around Z_B axis remains constant $\forall t \geq 0$. Thus, the kinematics model of the pan-tilt vision system can be reduced to

$$\dot{\mathbf{p}}_c = \begin{bmatrix} \dot{x}_c \\ \dot{y}_c \end{bmatrix} = \begin{bmatrix} -\dfrac{x_c y_c}{\alpha f} & \dfrac{x_c^2 + (\alpha f)^2}{\alpha f} \\ \dfrac{-y_c^2 - (\alpha f)^2}{\alpha f} & \dfrac{x_c y_c}{\alpha f} \end{bmatrix} \begin{bmatrix} \omega_T \\ \omega_P \end{bmatrix}, \tag{7}$$

in which $[\omega_T, \omega_P]^T \in \mathbb{R}^2$ are defined as the camera orientation velocities.

Change of variable

Before proceeding with system modeling, consider the following change of variable:

$$\begin{bmatrix} \omega_T \\ \omega_P \end{bmatrix} = \begin{bmatrix} 0 & -1 \\ 1 & 0 \end{bmatrix} \begin{bmatrix} \omega_x \\ \omega_y \end{bmatrix}. \tag{8}$$

Replacing the new vector of Eq. (8) in Eq. (7), we have that:

$$\dot{\mathbf{p}}_c = \begin{bmatrix} \dot{x}_c \\ \dot{y}_c \end{bmatrix} = \underbrace{\begin{bmatrix} \dfrac{x_c^2 + (\alpha f)^2}{\alpha f} & \dfrac{x_c y_c}{\alpha f} \\ \dfrac{x_c y_c}{\alpha f} & \dfrac{y_c^2 + (\alpha f)^2}{\alpha f} \end{bmatrix}}_{\mathbf{G}(\mathbf{p_c})} \underbrace{\begin{bmatrix} \omega_x \\ \omega_y \end{bmatrix}}_{\omega}. \tag{9}$$

The linear transformation in Eq. (8) was only chosen to reach a matrix format which is very useful in control system design. In fact, adopting such change of variable, the camera transformation matrix in Eq. (9) becomes uniformly symmetric and positive definite $\forall \mathbf{p_c}(t)$ as defined in (Slotine and Li, 1991, Page 80). In fact, we can verify that

$$[(x_c^2 + \alpha^2 f^2)/\alpha f] > 0\,, \qquad det[\mathbf{G}(\mathbf{p_c})] = (\alpha^2 f^2 + x_c^2 + y_c^2) > 0\,, \qquad \forall\, X_c, y_c\,.$$

Dynamics of DC motors

In order to compute the complete dynamical model of the pan-tilt mechanism, the dynamics of Pan and Tilt motors need to be considered. It is assumed in this work that the *Pan* and *Tilt* actuators are two DC-type motors, controlled by the armature voltages. In this case, the simplified dynamical equation for this actuators are well known in the literature and can be found in several textbooks, for instance in (Dorf and Bishop, 2009), namely:

$$\dot{\omega}_x = -k_1 \omega_x + k_2 V_x\,, \qquad \dot{\omega}_y = -k_1 \omega_y + k_2 V_y\,, \tag{10}$$

in which the subscribed indexes x and y stand for Pan and Tilt motors, respectively, as defined in (8). In Eq. (10), $\omega_x, \omega_y \in \mathbb{R}$ represent the speed of rotation of motors (in rad/s), the positive constants k_1, k_2 represent the combination of motors electromechanical parameters and $V_x, V_y \in \mathbb{R}$ represent the applied voltages (in Volts). Here, the motors are considered as of the same type, only for the sake of simplicity.

Pan-Tilt system model

Note that the control variables V_x, V_y in Eq. (10) are associated with time derivatives $\dot{\omega}_x, \dot{\omega}_y$. As it is intended to insert the dynamical equations of the motors into Eq. (9), an additional time differentiation is needed to obtain the complete model for the Pan-Tilt mechanism, namely:

$$\begin{cases} \ddot{\mathbf{p}}_\mathbf{c} = \mathbf{H}(\mathbf{p_c}, \dot{\mathbf{p}}_\mathbf{c})\omega \ + \ k_2 \mathbf{G}(\mathbf{p_c})\mathbf{V}\,, \\ \mathbf{H}(\mathbf{p_c}, \dot{\mathbf{p}}_\mathbf{c}) = \dot{\mathbf{G}}(\mathbf{p_c}) \ - \ k_1 \mathbf{G}(\mathbf{p_c})\,, \\ \mathbf{V} = [V_x; V_y]^T\,. \end{cases} \tag{11}$$

As can be seen from Eq. (11), the dynamics of target position $\mathbf{p_c}$, in the Pan-Tilt mechanism (the plant), exhibits a second order nonlinear behavior, with a time-varying matrix control gain $k_2 \mathbf{G}(\mathbf{p_c})$. In the next section, the control design for the system in Eq. (11) will be addressed for achieving tracking of moving targets. The control solution adopted is based on the linear version of the Active Disturbance Rejection Control (ADRC) method discussed in (Han, 1998; Madoński *et al.*, 2015).

CONTROL DESIGN - PROPOSED ADRC SCHEME

In this work, we define the system output error in image coordinates as $\mathbf{e_c} = \mathbf{p_c} - \mathbf{p_{cd}}$, with $\mathbf{p_{cd}} = [x_{cd}; y_{cd}]^T$ being the image projection of the desired position. Then, the error dynamics of the visual servoing Pan-Tilt mechanism will be given by:

$$\ddot{\mathbf{e}}_\mathbf{c} = \mathbf{H}(\mathbf{p_c}, \dot{\mathbf{p}}_\mathbf{c})\omega \; + \; k_2\mathbf{G}(\mathbf{p_c})\mathbf{V} \; - \; \ddot{\mathbf{p}}_\mathbf{cd}\,. \tag{12}$$

Output error dynamics

The design procedure adopted here is to produce a input/output transformation of the system error in Eq. (12) by introducing a constant gain $\beta \in \mathbb{R}$ in series with the output and a second order linear (stable) filter Q_0 in parallel with them, as depicted in Fig. 4. The real advantages of adopting such scheme will become clear later in this paper. As a general design procedure, the filter order is chosen to be the same as the plant order with $\alpha > 0$ for stability. In time domain, the output equation of the modified error dynamics can be written as:

$$\eta = [\eta_x \; ; \; \eta_y]^T = \beta\mathbf{e_c} + \mathbf{V_f}\,, \qquad \text{Filter } Q_0 \; : \; \ddot{\mathbf{V}}_\mathbf{f} \; = \; -\gamma_1\dot{\mathbf{V}}_\mathbf{f} - \gamma_0\mathbf{V_f} + \dot{\mathbf{V}}\,, \tag{13}$$

in which $\eta_x,\ \eta_y \in \mathbb{R}$ are the new error signals, $\mathbf{V_f}(t) \in \mathbb{R}^2$ is the filtered version of the control signal $\mathbf{V}(t) \in \mathbb{R}^2$, which is generated by the filter Q_0 (Fig. 4) with $(s+\alpha)^2 = s^2 + \gamma_1 s + \gamma_0$. By calculating the second order dynamics of the new error η based on Eq. (13), we obtain:

$$\ddot{\eta} = \beta\mathbf{H}(\mathbf{p_c}, \dot{\mathbf{p}}_\mathbf{c})\omega + \beta b\mathbf{G}(\mathbf{p_c})\mathbf{V} - \beta\ddot{\mathbf{p}}_\mathbf{cd} - \gamma_1\dot{\mathbf{V}}_\mathbf{f} - \gamma_0\mathbf{V_f} + \dot{\mathbf{V}}\,. \tag{14}$$

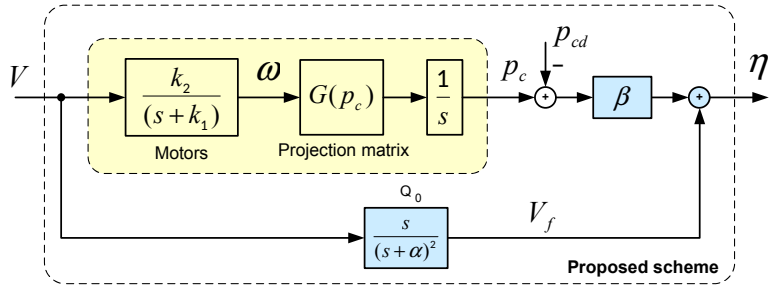

Figure 4 – Block diagram of the proposed (modified) ADRC scheme.

From the error expression in Eq. (13), we have that

$$\mathbf{V_f} = \eta - \beta\mathbf{e_c}\,, \qquad \dot{\mathbf{V}}_\mathbf{f} = \dot{\eta} - \beta\dot{\mathbf{e}}_\mathbf{c}\,. \tag{15}$$

After replacing Eq. (15) in the error dynamics of Eq. (14), we obtain

$$\ddot{\eta} + \gamma_1\dot{\eta} + \gamma_0\eta \; = \; \beta\mathbf{H}(\mathbf{p_c}, \dot{\mathbf{p}}_\mathbf{c})\omega + \beta b\mathbf{G}(\mathbf{p_c})\mathbf{V} - \beta\ddot{\mathbf{p}}_\mathbf{cd} + \gamma_1\dot{\mathbf{e}}_\mathbf{c} + \gamma_0\mathbf{e_c} + \dot{\mathbf{V}}\,, \tag{16}$$

which can be represented in a more compact form, such as:

$$\ddot{\eta} + \gamma_1\dot{\eta} + \gamma_0\eta \; = \; \psi(t) + \dot{\mathbf{V}}\,, \tag{17}$$

$$\psi(t) = \; \beta\mathbf{H}(\mathbf{p_c}, \dot{\mathbf{p}}_\mathbf{c})\omega + \beta b\mathbf{G}(\mathbf{p_c})\mathbf{V} - \beta\ddot{\mathbf{p}}_\mathbf{cd} + \gamma_1\dot{\mathbf{e}}_\mathbf{c} + \gamma_0\mathbf{e_c}\,. \tag{18}$$

As also done in the ADRC basic formalism (Han, 1998; Madoński *et al.*, 2015), the term $\psi(t)$ is denoted here as the system *generalized or total disturbance*. Its is important to emphasize that the disturbance term $\psi(t)$ gathers together the plant uncertainties, nonlinearities, unmodeled dynamics, non measurable signals and/or non measurable state variables.

Remark 1 *The key advantage of introducing a linear filter Q_0 in parallel with the system in Eq. (12) is the derivation of a (new) linear stable plant in Eq. (17), that is subjected to a disturbance term $\psi(t)$ and to an (new) input signal $\dot{\mathbf{V}}$ with identity matrix control gain.*

Control law definition

Another advantage of the proposed scheme detached in the previous section is that the control signal of the system in Eq. (17) are decoupled. That means the control design for both η_x and η_y dynamics can be carried out separately. Then, from Eqs. (17),(18), we can write:

$$\begin{cases} \ddot{\eta}_x = -\gamma_1 \dot{\eta}_x - \gamma_0 \eta_x + \psi_x + \dot{V}_x\,, \\ \ddot{\eta}_y = -\gamma_1 \dot{\eta}_y - \gamma_0 \eta_y + \psi_y + \dot{V}_y\,. \end{cases} \qquad [\psi_x\,;\,\psi_y]^T \;=\; \psi(t)\,, \tag{19}$$

Since the internal dynamics of both η_x and η_y errors are stable, then simple and viable control laws for them could be given by:

$$\dot{V}_x = -\psi_x\,, \qquad \dot{V}_y = -\psi_y\,, \tag{20}$$

unless for the fact that ψ_x and ψ_y are not available quantities. In order to overcome such implementation difficulty, the ADRC methodology proposes the use of an extended state observed (ESO) in which such disturbance terms are considered as additional system states to be estimated. Thus, by defining the system states as $z = [\eta_x,\ \dot{\eta}_x,\ \psi_x]^T$ and $q = [\eta_y,\ \dot{\eta}_y,\ \psi_y]^T$, the corresponding state space representations will be given by:

$$\dot{z} = \underbrace{\begin{bmatrix} 0 & 1 & 0 \\ -\gamma_0 & -\gamma_1 & 1 \\ 0 & 0 & 0 \end{bmatrix}}_{A} z + \underbrace{\begin{bmatrix} 0 \\ 1 \\ 0 \end{bmatrix}}_{B} \dot{V}_x + \underbrace{\begin{bmatrix} 0 \\ 0 \\ 1 \end{bmatrix}}_{\Lambda} \dot{\psi}_x\,, \qquad \dot{q} = \begin{bmatrix} 0 & 1 & 0 \\ -\gamma_0 & -\gamma_1 & 1 \\ 0 & 0 & 0 \end{bmatrix} q + \begin{bmatrix} 0 \\ 1 \\ 0 \end{bmatrix} \dot{V}_y + \begin{bmatrix} 0 \\ 0 \\ 1 \end{bmatrix} \dot{\psi}_y\,,$$

$$z_1 = \underbrace{\begin{bmatrix} 1 & 0 & 0 \end{bmatrix}}_{C} z, \qquad\qquad q_1 = \begin{bmatrix} 1 & 0 & 0 \end{bmatrix} q\,. \tag{21}$$

As can be noticed from Eq. (21), the pair (A,C) is *observable* and then the ESOs design can be carried out without restrictions. Thus, based on Eq. (21), we define the following observers' states: $\hat{z} = [\hat{z}_1,\ \hat{z}_2,\ \hat{z}_3]^T$ and $\hat{q} = [\hat{q}_1,\ \hat{q}_2,\ \hat{q}_3]^T$, which are governed by:

$$\dot{\hat{z}} = \begin{bmatrix} 0 & 1 & 0 \\ -\gamma_0 & -\gamma_1 & 1 \\ 0 & 0 & 0 \end{bmatrix} \hat{z} + \begin{bmatrix} 0 \\ 1 \\ 0 \end{bmatrix} \dot{V}_x + \underbrace{\begin{bmatrix} L_1 \\ L_2 \\ L_3 \end{bmatrix}}_{L} \varepsilon_x\,, \qquad \dot{\hat{q}} = \begin{bmatrix} 0 & 1 & 0 \\ -\gamma_0 & -\gamma_1 & 1 \\ 0 & 0 & 0 \end{bmatrix} \hat{q} + \begin{bmatrix} 0 \\ 1 \\ 0 \end{bmatrix} \dot{V}_y + \begin{bmatrix} L_1 \\ L_2 \\ L_3 \end{bmatrix} \varepsilon_y\,,$$

$$\hat{z}_1 = \begin{bmatrix} 1 & 0 & 0 \end{bmatrix} \hat{z}, \qquad \varepsilon_x = z_1 - \hat{z}_1\,, \qquad\qquad \hat{q}_1 = \begin{bmatrix} 1 & 0 & 0 \end{bmatrix} \hat{q}, \qquad \varepsilon_y = q_1 - \hat{q}_1\,. \tag{22}$$

where $\varepsilon_x, \varepsilon_y \in \mathbb{R}$ denotes the ESOs' output errors and $L_1, L_2, L_3 \in \mathbb{R}$ are the observer gains, usually chosen to satisfy the stable polynomial $(s+w_0)^3 = s^3 + L_1 s^2 + L_2 s + L_3$, with $w_0 > 0$. The design constant w_0 stands for the stable characteristic roots of the ESOs in Eq. (22) whose absolute value is directly related to their estimation velocity (and bandwidth). By assuming that w_0 is conveniently chosen, then L_1, L_2, L_3 will be well defined and the ESOs' error dynamics will be given by:

$$\dot{e}_z = \underbrace{(A - LC)}_{A_m} e_z + \Lambda \dot{\psi}_x\,, \qquad \dot{e}_q = (A - LC)\, e_q + \Lambda \dot{\psi}_y\,,$$
$$\varepsilon_x = C\, e_z\,, \qquad\qquad \varepsilon_y = C\, e_q\,, \tag{23}$$

in which $e_z = [e_{z1}, e_{z2}, e_{z3}]^T = [(\eta_x - \hat{z}_1), (\dot{\eta}_x - \hat{z}_2), (\psi_x - \hat{z}_3)]^T$, $e_q = [e_{q1}, e_{q2}, e_{q3}]^T = [(\eta_y - \hat{q}_1), (\dot{\eta}_y - \hat{q}_2), (\psi_y - \hat{q}_3)]^T$. Thus, assuming that the ESOs are sufficiently fast and precise, the control laws for the system (19) can be chosen based on the estimated states, that is:

$$\dot{V}_x = -\hat{z}_3\,, \qquad \dot{V}_y = -\hat{q}_3\,. \tag{24}$$

STABILITY ANALYSIS

By replacing the control law expression of Eq. (24) into Eq. (19), the closed loop dynamics for the error $\eta(t)$ becomes:

$$\ddot{\eta} + \gamma_1 \dot{\eta} + \gamma_0 \eta = [e_{z3}, e_{q3}]^T\,, \tag{25}$$

Since the components of the vector function on the left-hand side of (25) correspond to a linear, time-invariant and stable ODE, then bounded ESO errors $[e_{z3}, e_{q3}]^T$ will result in a bounded $\eta(t)$. Provided that the boundedness and convergence properties of the closed loop signals in (25) are dependent on the ESO (23) estimation error, an investigation about them is needed. To verify the influence of the generalized disturbance terms (19) in the amplitude of the observer estimation error in (23), let us compute the transfer function from ψ_x to e_{z3} and from ψ_y to e_{q3}, by using:

$$G(s) = C_\Omega (sI - A_m)^{-1} \Lambda, \quad \text{with} \quad C_\Omega = [0\ 0\ 1]\,. \tag{26}$$

From Eqs. (26),(23), it is not difficult to verify that

$$G(s) = \begin{bmatrix} 0 & 0 & 1 \end{bmatrix} \begin{bmatrix} (s+L_1) & -1 & 0 \\ L_2+\gamma_0 & s+\gamma_1 & -1 \\ L_3 & 0 & s \end{bmatrix}^{-1} \begin{bmatrix} 0 \\ 0 \\ 1 \end{bmatrix}, \tag{27}$$

$$s^3 + (L_1+\gamma_1)s^2 + (\gamma_1 L_1 + L_2 + \gamma_0)s + L_3 = (s+\omega_0)^3, \tag{28}$$

which results in:

$$G(s) = \left[1 - \frac{\omega_0^3}{(s+\omega_0)^3}\right], \qquad e_{z3} = G(s)\psi_x, \qquad e_{q3} = G(s)\psi_y, \tag{29}$$

Remark 2 *Here, it is important to mention that the adoption of the mixed representation for both time and frequency domain quantities in (29) is only for analysis purpose. As we intend to investigate the magnitude of the estimation errors e_{z3}, e_{q3}, we believe it is the most suitable input/output mathematical formalism to be utilized, in the present analysis, provided that the terms ψ_x, ψ_y involve nonlinear functions of the plant states, which may prevent its representation in the frequency domain.*

Remark 3 (ESO precision) *By manipulating the state errors definitions in Eq. (23) together with Eq. (29), we verify that*

$$\hat{z}_3 = \frac{\omega_0^3}{(s+\omega_0)^3}\ \psi_x, \qquad \hat{q}_3 = \frac{\omega_0^3}{(s+\omega_0)^3}\ \psi_y, \tag{30}$$

which reveal that the estimation precision of ESOs can be increased arbitrarily by choosing sufficiently large absloute values for the characteristic roots ω_0.

SIMULATION RESULTS

In this section, we present and discuss simulation of the proposed ADRC scheme applied to the Pan-Tilt camera mechanism. For the simulation, the dynamics of the overall control system composed by: (i) the mechanism in Eq. (14), (ii) the extended observers (ESOs) in Eq. (22), (iii) the filter Q_0 in Eq. (13), and the control laws based on Eq. (24), were all coded using Simulink^{TM} block programing. The simulation sample time was 0.001 s. The curves in Fig. 5 illustrate the performance of the proposed ADRC strategy applied in the tracking control problem in which the reference signal is given by $p_{cd} = [210 + 100sin(t); 70 + 100cos(0.5t)]^T$ [pixels]. As can be deduced from Fig. 5, the output tracking errors converge to a small residual region close to zero.

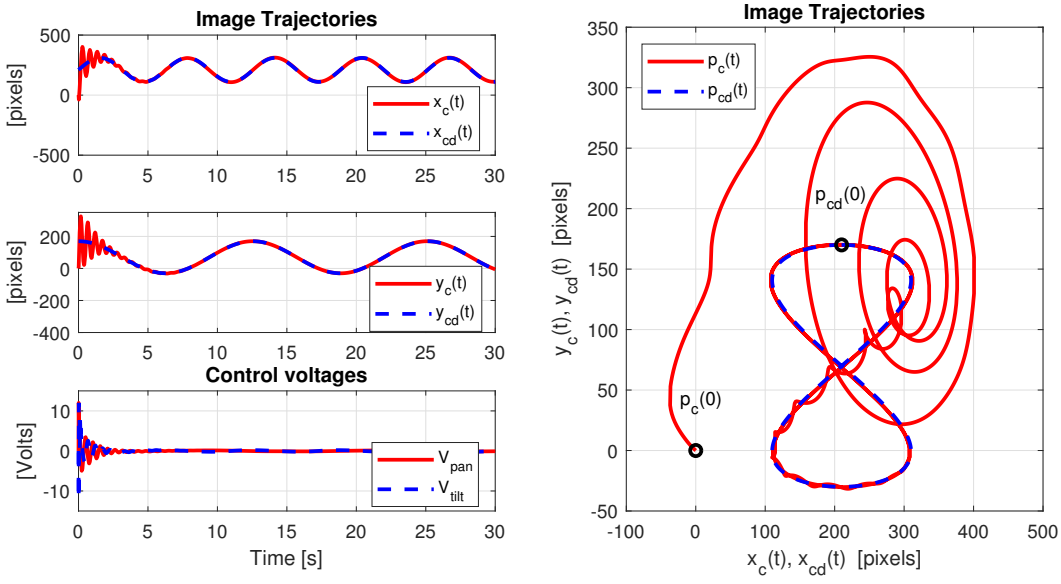

Figure 5 – Simulation results. Lissajous curve tracking case.

CONCLUSION

In this work, an extension of the ADRC controller for a pan-tilt visual servoing mechanism for tracking a moving target was developed. To solve the problem of uncertainties in the system control coefficient, a modification in the basic

ADRC method. It consisted in the introduction of a constant gain in series with the system output error, and a linear filter in parallel with the plant. The objective was to produce an input/output system which was equivalent to the original one but with a known control coefficient, while keeping the original control objective. An interesting feature of the proposed strategy was the relaxation of the requirement of exact knowledge of the plant control coefficient, which contrasts with other works in this field. The stability and convergence properties of the closed loop system were demonstrated by numerical simulation.

REFERENCES

Bista, S.R., Giordano, P.R. and Chaumette, F., 2017. "Combining line segments and points for appearance-based indoor navigation by image based visual servoing". In *Intelligent Robots and Systems (IROS), 2017 IEEE/RSJ International Conference on*. IEEE, pp. 2960–2967.

Chen, H., Zhao, X. and Tan, M., 2014. "A Novel Pan-tilt Camera Control Approach for Visual Tracking". In *Proceedings of the 2014 11th World Congress on Intelligent Control and Automation*. Shenyang, China, pp. 2860–2865.

Dorf, R.C. and Bishop, R.H., 2009. *Sistemas de Controle Modernos*. Livros Técnicos e Científicos.

Feng, H., Lu, Y., Chen, D., Ma, T. and Fu, Y., 2018. "Development on a magnetic anchoring robot system based on visual servo control for laparoendoscopic single-site surgery". *The International Journal of Medical Robotics and Computer Assisted Surgery*, p. e1904.

Flandin, G., Chaumette, F. and Marchand, E., 2000. "Eye-in-hand/Eye-to-hand Cooperation for Visual Servoing". In *Proceedings of the 2000 IEEE International Conference on Robotics and Automation*. San Francisco, CA, USA, Vol. 3, pp. 2741–2746.

Han, J., 1998. "Auto-disturbance rejection control and its applications". *Control and Decision*, Vol. 13, No. 1, pp. 19–23.

He, H., Lai, R., Li, J., Liu, X., Zhu, L., Feng, M. and Shao, L., 2017. "Rotation-traction manipulation bionic training robot based on visual servo and impedance control". In *Mechatronics and Automation (ICMA), 2017 IEEE International Conference on*. IEEE, pp. 1781–1786.

Hutchinson, S., Hager, G.D. and Corke, P.I., 1996. "A Tutorial on Visual Servo Control". *IEEE Transactions on Robotics and Automation*, Vol. 12, No. 5, pp. 651–670.

Kelly, R., Carelli, R., Nasisi, O., Kuchen, B. and Reyes, F., 2000. "Stable Visual Servoing of Camera-in-hand Robotic Systems". *IEEE/ASME Transactions on Mechatronics*, Vol. 5, No. 1, pp. 39–48.

Li, L., Wang, B., Li, B., Xiao, P., Wang, W. and Li, Y., 2013. "The Application of Image based Visual Servo Control System for Smart Guard". In *Proceedings of the 2013 10th IEEE International Conference on Control and Automation*. Hangzhou, China, pp. 1342–1345.

Madoński, R., Gao, Z. and Łakomy, K., 2015. "Towards a turnkey solution of industrial control under the active disturbance rejection paradigm". In *54th Annual Conference of the Society of Instrument and Control Engineers of Japan (SICE)*. IEEE, pp. 616–621.

Masten, M.K., 2008. "Inertially Stabilized Platforms for Optical Imaging Systems". *IEEE Control Systems*, Vol. 28, No. 1, pp. 47–64.

Paucar, C., Morales, L., Pinto, K., Sánchez, M., Rodríguez, R., Gutierrez, M. and Palacios, L., 2018. "Use of drones for surveillance and reconnaissance of military areas". In *International Conference of Research Applied to Defense and Security*. Springer, pp. 119–132.

Siciliano, B., Sciavicco, L., Villani, L. and Oriolo, G., 2008. *Robotics: Modelling, Planning and Control*. Advanced Textbooks in Control and Signal Processing. Springer-Verlag London Ltd.

Sivčev, S., Rossi, M., Coleman, J., Dooly, G., Omerdić, E. and Toal, D., 2018. "Fully automatic visual servoing control for work-class marine intervention rovs". *Control Engineering Practice*, Vol. 74, pp. 153–167.

Slotine, J.J. and Li, W., 1991. *Applied Nonlinear Control*. Prentice Hall.

Vijayan, A.T. and Ashok, S., 2017. "Integrating visual guidance and feedback for an industrial robot". In *Control and Robotics Engineering (ICCRE), 2017 2nd International Conference on*. IEEE, pp. 18–22.

Zhao, C. and Huang, Y., 2012. "Adrc based input disturbance rejection for minimum-phase plants with unknown orders and/or uncertain relative degrees". *Journal of Systems Science and Complexity*, Vol. 25, No. 4, pp. 625–640.